

1 *Title Page*

2 **Title: Contributions of cryptochromes and phototropins to stomatal opening through**
3 **the day**

4 Authors: Fang Wang ¹, T. Matthew Robson ¹, Jorge J. Casal ^{2,3}, Alexey Shapiguzov ^{1,4}, Pedro
5 J. Aphalo ^{1*}

6 1. Viikki Plant Science Centre (ViPS), Department of Biosciences, Faculty of Biological
7 and Environmental Sciences, University of Helsinki, 00014, Finland

8 2. IFEVA, Facultad de Agronomía, Universidad de Buenos Aires and CONICET, Av. San
9 Martín 4453, 1417 Buenos Aires, Argentina

10 3. Fundación Instituto Leloir, Instituto de Investigaciones Bioquímicas de Buenos Aires–
11 CONICET, 1405 Buenos Aires, Argentina

12 4. Permanent address: Institute of Plant Physiology, Russian Academy of Sciences,
13 Botanicheskaya Street, 35, 127276 Moscow, Russia

14 * Corresponding author: pedro.aphalo@helsinki.fi

15

16 **Summary (80/80 words)**

17 We studied the times of day at which cryptochromes and phototropins participate in stomatal
18 responses to light, by subjecting *Arabidopsis* mutants in these two photoreceptors to 11-hour
19 exposure to blue-, red- or green-light. Under blue light, phototropins had relatively greater
20 importance at the start of the photoperiod, whereas cryptochromes were important for stomatal
21 opening throughout the photoperiod. This different timing of contributions by two families of
22 photoreceptors to stomatal opening indicates that the mechanism is more complicated than usually
23 assumed.

24 **Abstract (196/200 words)**

25 The UV-A/blue photoreceptors phototropins and cryptochromes are both known to contribute to
26 stomatal opening (Δg_s) in blue light. However, their relative contributions to maintenance of g_s in
27 blue light through the whole photoperiod remains unknown. To elucidate this question,
28 *Arabidopsis phot1 phot2* and *cry1 cry2* mutants (MTs) and their respective wild types (WTs) were
29 irradiated with $200 \mu\text{mol m}^{-2} \text{s}^{-1}$ of blue-, green- or red-light (BL, GL or RL) throughout a 11-hour
30 photoperiod. Stomatal conductance (g_s) was higher under BL, than under RL or GL. Under RL, g_s
31 was not affected by either of the photoreceptor mutations, but under GL g_s was slightly lower in
32 *cry1 cry2* than its WT. Under BL, the presence of phototropins was essential for rapid stomatal
33 opening at the beginning of the photoperiod, while maximal stomatal opening beyond 3 h of
34 irradiation required both phototropins and cryptochromes. Time courses of whole-plant net carbon
35 assimilation rate (A_{net}) and the effective quantum yield of photosystem II photochemistry (ΦPSII)
36 were consistent with an A_{net} -independent contribution of BL on g_s both in *phot1 phot2* and *cry1*
37 *cry2* mutants. The changing roles of phototropins and cryptochromes through the day may allow
38 more flexible coordination between g_s and A_{net} .

39 **Keywords (max 10)**

40 *Arabidopsis thaliana*; blue light; diurnal pattern; gas exchange; green light; photosynthesis; red
41 light; stomata;

42 **Introduction**

43 The major function of leaf stomata is to open for photosynthetic carbon fixation and to close for
44 the avoidance of dehydration. This function is a compromise, determined by internal as well as
45 environmental factors and tightly related to the photosynthetic carbon metabolism (Cowan and
46 Farquhar 1977). Light is the ultimate energy source for plant growth, and one of the most important
47 environmental cues for stomatal opening. Indoor experiments have verified that different light
48 qualities stimulate stomatal opening (Sharkey and Raschke 1981; Shimazaki *et al.* 2007). Blue
49 light (BL) is the most effective band of the visible spectrum inducing stomatal opening even at
50 irradiances as low as $1 \mu\text{mol m}^{-2} \text{s}^{-1}$ and this BL-specific stomatal opening is considered as
51 independent on photosynthesis (A_{net}) (Shimazaki *et al.* 2007), whereas stomatal opening driven by
52 red light (RL) is thought to depend on photosynthetic metabolism (e.g. Sharkey and Raschke 1981;
53 Wang *et al.* 2011). A well-documented link exists between net carbon assimilation rate in the
54 mesophyll A_{net} and stomatal conductance (g_s) through depletion of CO_2 concentration in the leaf
55 intercellular air spaces (C_i) by A_{net} and the opening response of stomata to a decrease in C_i (e.g.
56 Aphalo and Jarvis 1993; Roelfsema *et al.* 2002). However, it has also been shown that C_i does not
57 always fully explain stomatal opening under RL and the involvement of signals different from C_i
58 has been suggested to also link g_s and A_{net} (reviewed by Lawson *et al.* 2010; Matthews *et al.* 2017).
59 In addition, as stomata in epidermal peels open under RL in the absence of mesophyll, guard cell
60 A_{net} may also contribute to stomatal opening (Matthews *et al.* 2017; Shimazaki *et al.* 2007). Like
61 RL, BL also penetrates the epidermis and drives photosynthesis in the mesophyll. Thus, direct
62 stomatal opening in response to BL perceived through photoreceptors and indirect
63 photosynthetically driven opening are both involved in BL-induced stomatal opening when
64 irradiance is not weak (Sharkey and Ogawa 1987). Compared with BL- and RL-induced responses,
65 stomatal opening induced by green light (GL) has been studied less frequently, and findings have
66 been inconsistent among studies. GL is generally considered to be less effective in opening stomata
67 than RL, and much less effective than BL (Sharkey and Raschke 1981; Folta and Maruhnich 2007),
68 and also able to reverse stomatal opening induced by BL under a background of RL (Frechilla *et*
69 *al.* 2000; Talbott *et al.* 2002).

70 Cryptochromes (crys) and phototropins (phots) are both flavoprotein photoreceptors with different
71 protein structures activated by radiation spanning the ultraviolet-A (UVA) and BL (Banerjee and

72 Batschauer 2005; Christie *et al.* 2015). Both of crys and phots absorb *in vitro* mainly UV and BL
73 when dark adapted, while, when light-adapted, crys but not phots strongly absorb GL in addition
74 to UV and BL (Banerjee *et al.* 2007; Christie *et al.* 2015). Crys are known to be involved in the
75 inhibition of hypocotyl elongation, entrainment of the circadian rhythm, stomatal opening and
76 shade avoidance (Sellaro *et al.* 2010; Chen *et al.* 2012; Sellaro *et al.* 2012), while phots are
77 implicated in the control of phototropism, chloroplast movement, leaf expansion and movement
78 (Briggs and Huala 1999; Christie 2007). Certain roles in photomorphogenic processes have been
79 attributed to crys and phots based on the comparison of gene expression, molecular pathways and
80 biochemical functions that they promote (Briggs and Huala 1999; Liscum *et al.* 2003; Ohgishi *et*
81 *al.* 2004). In the regulation of stomatal responses, phots seem to be dominant in rapid stomatal
82 response to BL at a low fluence rate (Shimazaki *et al.* 2007; Chen *et al.* 2012), while crys regulate
83 stomatal opening at relatively high irradiances of BL and also could affect g_s under background
84 RL (Talbot *et al.* 2003; Boccalandro *et al.* 2012). Phots are reported to ultimately activate the
85 plasma membrane H^+ -ATPase that drives K^+ uptake leading to increased turgor pressure and
86 stomatal opening (Inoue *et al.* 2010). Crys have been shown to interact with CONSTITUTIVE
87 PHOTOMORPHOGENIC1 (COP1) (Shimazaki *et al.* 2007) in circadian-rhythm regulation
88 (Briggs and Huala 1999). Kinoshita *et al.* (2011) found a possible link between phot-mediated
89 stomatal responses to BL and the circadian clock through *FLOWERING LOCUS T* (FT), whereas
90 Ando *et al.* (2013) using epidermal peels provide evidence for cry affecting stomatal opening
91 through FT and the circadian clock.

92 Tenhunen *et al.* (1987) studied stomatal function by following daily patterns of gas exchange in
93 various natural environments, concluding that the coupled relationship between g_s and A_{net} is
94 important in leaf function over a diurnal period. Various studies have attempted to identify the
95 underlying mechanism behind these diurnal patterns. Talbot and Zeiger (1996) explored a model
96 of osmoregulation driving stomatal diurnal movements under white light (WL), since potassium
97 ions (K^+) were found to be the predominant guard-cell osmoticum during the first half of the day
98 and sugars (sucrose and malate) in the second half of the day. This model was extended by Tallman
99 (2004) to incorporate regulation of diurnal stomatal movements by dual-source-controlled
100 fluctuations in ABA metabolism. The dynamics of stomatal regulation in whole plants are poorly
101 understood and Matthews *et al.* (2017) recommend that future research takes them into
102 consideration. While crys and phots are known to induce stomatal opening (Chen *et al.* 2012), their

103 contribution towards the regulation of diurnal patterns of stomatal opening themselves, and
104 through interaction with other established mechanisms of stomatal control, have not been
105 elucidated. Here we aim to answer the following two questions:

- 106 a) Are diurnal patterns in g_s correlated with diurnal patterns in A_{net} under blue, green and red
107 monochromatic light? Lack of correlation would imply that mechanisms independent of
108 A_{net} , likely attributable to photoreceptors, make an important contribution to light-induced
109 g_s through the photoperiod.
- 110 b) Are the roles of the BL photoreceptors *crys* and *phots* in stomatal opening different and do
111 they vary during the photoperiod? Such differences would imply that these photoreceptors
112 contribute to determining the shape of diurnal patterns of g_s .

113 To answer these questions, we concurrently measured the diurnal time courses of g_s , A_{net} and C_i in
114 *Arabidopsis thaliana* double mutant types (MTs) *phot1 phot2* and *cry1 cry2* and their wild types
115 (WTs) under constant irradiance of RL, GL or BL, or in darkness.

116 **Material and Methods**

117 Plant materials and growth conditions

118 *Arabidopsis thaliana* double MT *phot1-5 phot2-1* and its WT Columbia-5 (alias Col-0 *gll-1*,
119 glabrous derivative of Col-0, shortened to Col-5), and double MT *cry1-1 cry2-1* and its WT
120 Landsberg *erecta* (*Ler*) were employed in the experiments. For a given replicate, seeds of all
121 genotypes were produced at the same time, by plants grown side-by-side. Seeds were sown in
122 square plastic 70- \times -70-mm pots filled with a substrate composed of 50% pre-fertilised-and-limed
123 peat and 50% vermiculite. The sown pots were kept at 4 °C in darkness for two days and three
124 nights, and then moved to a controlled-environment walk-in growth room.

125 After one week's growth, each single plant was transplanted into a pot (60 mm in diameter and 47
126 mm in height) into the same substrate as used for germination and continued to grow in a walk-in
127 growth room for three weeks. Gas exchange measurements were made on these single seedlings.
128 Given that only one plant could be measured per day, a cohort of plants was grown each week to
129 produce a continuous supply of equivalent plants. For chlorophyll fluorescence measurements,
130 seedlings were transplanted into trays of 3- \times -2 cells. Each cell was 45- \times -55 mm across and 60 mm

131 deep. A balanced design was used to arrange the genotypes in the trays, with different genotypes
132 spatially interspersed and their positions randomised.

133 In the growth room, fluorescent tubes (L 58W/865 LUMILUX, OSRAM, Germany) supplied a
134 constant photon irradiance of $205 \pm 15 \mu\text{mol m}^{-2} \text{s}^{-1}$ PAR (mean \pm s.e., see Fig. SI1 for spectra),
135 with a 12 h photoperiod from 7.00 a.m. (ZT = 00:00, expressed in hours and minutes) to 7.00 p.m.
136 Air relative humidity and air temperature, next to the growing plants, were recorded by three
137 DS1923 Hygrochron temperature/humidity data loggers (iButtons, Maxim Integrated, San Jose,
138 CA, U.S.A). Relative humidity (RH) was $67 \pm 0.4\%$ / $74 \pm 0.5\%$ (mean \pm SE) day / night and
139 temperature (T) was $22 \pm 0.03 \text{ }^\circ\text{C}$ / $20 \pm 0.05 \text{ }^\circ\text{C}$ (mean \pm SE) day / night.

140 Gas exchange measurements

141 *Light treatments*

142 A custom-built light source based on three-colour LED arrays was used. The light source consisted
143 of two RGB LED arrays (Red-Green-Blue 90 Die Hex type NHXRGB090S00S, Norlux, Chicago,
144 USA) assembled on a $120 \times 100 \times 35$ (L \times W \times H) mm passive heat sink. The spectral photon
145 irradiance for the three channels is given in Fig. SI2A and the actual light-source is shown in Fig.
146 SI2B. The gap between the top of the chamber and the light source 30-mm above was sealed with
147 high-density black foam to block room-light from entering the chamber. The foam was covered
148 on the inside by a high-reflectance-plastic white-reflection standard card (Zebra check card,
149 Novoflex, Memmingen, Germany) to improve light-field evenness. The light source was powered
150 by three programmable power supplies (GW INSTEK PSP-2010, New Taipei City, Taiwan China)
151 in constant current mode. The current setting was adjusted to achieve an irradiance of $200 \mu\text{mol m}^{-2}$
152 s^{-1} measured with the built-in sensor of the gas-exchange chamber at the time when each plant
153 was enclosed; irradiance remaining in all cases within $\pm 10\%$ of the set value for the whole day.
154 One power source was used to control each colour channel in both arrays. Each power supply was
155 switched on at ZT = 00:00 (7 a.m.) and off at ZT = 11:30 (6.30 p.m.) by a program running on a
156 computer. For the experiments reported here, only one single-colour channel was used at a time.
157 The cuvette was darkened for the whole day in the darkness treatments by covering its top with
158 the darkening plate provided as part of the gas-exchange system.

159 A portable gas exchange system GFS-3000 with Arabidopsis whole-plant Chamber 3010-A (GFS,
160 Walz, Effeltrich, Germany) was used to measure transpiration, A_{net} , C_i and g_s . Settings were 750
161 $\mu\text{mol s}^{-1}$ air flow rate, level 5 impeller speed, 390 ppm ambient CO_2 (C_a), 22 °C cuvette air
162 temperature and 67% relative humidity. The average leaf temperature was stable before and during
163 the light treatments at 21.69 °C – 21.86 °C (SI Script). The actual values of C_a accounting for any
164 deviation from the set value are given in Table S11. Plants were enclosed in the *Arabidopsis* cuvette
165 for 22 to 23 h. Drift in ambient conditions and bias in measurements were avoided by regular
166 IRGA re-zeroing. The chamber was under excess pressure, adjusted by means of its vent valve at
167 the bottom of the pot compartment. This coupled with a collar of white polyethylene film covering
168 the surface of the soil prevented soil respiration and evaporation from interfering with the
169 measurement of shoot gas exchange.

170 The order in which treatments and genotypes were measured was fully randomized to avoid bias,
171 including bias caused by the age differences between plants within the weekly cohorts. So as to
172 ensure consistency, settings and the measurement protocol were stored as a program and ran
173 uninterrupted for 22-23 h during each measurement session using the GFS-Win (Walz) program
174 on a computer (different from the one for the light power supply). Each measurement cycle started
175 with one IRGA re-zeroing, followed by acquisition of 4 data records and ended with another IRGA
176 re-zeroing followed by an interval until the start of the next cycle, on a 33-36 min loop (SI Script).
177 The measuring protocol consisted of enclosing a plant in the cuvette the previous evening at
178 approximately 6:30 p.m. (ZT = -12:30), immediately after transfer from the growth room to an
179 adjacent laboratory. The enclosed plant remained in darkness, under the conditions indicated above,
180 until the next morning, when at 7 a.m. (ZT = 00:00) one of the colour channels of the light source
181 was switched on (except in the darkness treatment). The data collected per plant at 147 or more
182 time points between midnight (ZT = -07:00) and 6.30 p.m. (ZT = 11:30) were checked for any
183 anomalies.

184 Delta stomatal conductance (Δg_s) was calculated as the difference between each g_s value measured
185 during the photoperiod and g_s measured in darkness on the same plant at the last time-point before
186 the start of the photoperiod. This calculated Δg_s allowed for more precise analysis of the
187 differences between genotypes because it enabled a correction to be made for differences in
188 baseline values of g_s in darkness among individual plants. The C_i was expressed as a fraction of

189 C_a . to minimize any effect of slight fluctuations in C_a (Table SII). Raw g_s data are presented in Fig.
190 SI3, A_{net} in Fig. SI4 and C_i/C_a in Fig. SI5.

191 *Leaf area calculation*

192 As whole plants were measured, calculation of gas-exchange rates expressed per unit area required
193 the estimation of the enclosed illuminated leaf area. The projected rosette area was used as a proxy
194 for the illuminated leaf area. The plant was taken from the growth room before the end of the
195 photoperiod (*ca.* 6.30 p.m.) when leaves were horizontal in all genotypes. Next, as mentioned
196 above, a collar of white polyethylene film was placed below the rosette covering the soil, providing
197 a contrasting background for the photographs and subsequently photographed on a copy stand
198 alongside an identical empty pot covered with a black square pattern drawn on a white background
199 used as a reference (NIKON D100, AF NIKKOR 50MM f/1.8D, Japan). ImageJ (Schneider *et al.*
200 2012) was employed to estimate the whole rosette projected area (Wang 2017). The average
201 projected rosette area of individual plants used for gas exchange measurements was $457 \pm 2 \text{ mm}^2$
202 in WT Col-5, $413 \pm 2 \text{ mm}^2$ in its MT *phot1 phot2*, $511 \pm 3 \text{ mm}^2$ in WT *Ler*, and $518 \pm 2 \text{ mm}^2$ in
203 its MT *cry1 cry2* (mean \pm s.e.).

204 In a subset of plants of each genotype, the total area of all the leaves was measured in addition to
205 the rosette area to assess overlap among leaves, given that the leaves were nearly horizontal when
206 sampled during the photoperiod. All leaves were excised at the base of the petiole, leaf blades held
207 flat to avoid curling, photographed and quantified in the same way as rosette projected area. The
208 relationships between rosette projected area and the total leaf area estimates were: $88 \pm 6 \%$ in WT
209 Col-5 and $62 \pm 3 \%$ in its MT *phot1 phot2*, $94 \pm 2 \%$ in WT *Ler* and $90 \pm 4 \%$ in its MT *cry1 cry2*
210 (mean \pm s.e.).

211 Chlorophyll fluorescence measurements

212 IMAGING-PAM M-Series (Walz, Effeltrich, Germany) was employed to make chlorophyll
213 fluorescence measurements. These were performed in a darkened purpose-built cubicle located
214 within a large well-ventilated hall, with *c* 500 ppm C_a and *c* 30 % RH. Four plants of each of the
215 four genotypes were measured simultaneously in one tray, each tray being a true replicate or block.
216 The blue LED (450 nm, $230 \mu\text{mol m}^{-2} \text{ s}^{-1}$) built-into the IMAGING-PAM was kept on from 7.00
217 a.m. (ZT = 00:00) until 5.00 p.m. (ZT = 10:00). Irradiance was measured at the level of the

218 seedlings at the centre of the tray. The following protocol was used to obtain a diurnal time course
219 of the effective quantum yield of photosystem II photochemistry (Φ PSII). Against the background
220 of continuous actinic light ($230 \mu\text{mol m}^{-2} \text{s}^{-1}$ above the rosette, measured with a LI-250A light
221 meter – LI-COR, Lincoln, Nebraska, USA), the low-intensity measuring light was triggered once
222 every two minutes throughout the experiment to probe steady-state fluorescence under
223 illumination (F_s). Saturating light pulses ($5000 \mu\text{mol m}^{-2} \text{s}^{-1}$, duration of 1 s from an LED-Array
224 Illumination Unit IMAG-MAX/L) were triggered once every 10 min to measure maximal
225 fluorescence under illumination (F_m'). Φ PSII was calculated as $(F_m' - F_s)/F_m'$ (Genty *et al.*, 1989).
226 The measuring light was of intensity 2 and frequency 1 set in Walz Imaging Win Software. The
227 programmed protocol can be checked in SI Script.

228 Stomatal density and size

229 Two young fully-expanded leaves were collected from each of 10 plants per genotype grown under
230 the same conditions as the plants used for gas exchange for the purpose of making comparisons of
231 stomatal density and size. These two leaves were painted with clear nail varnish, one on the adaxial
232 side and the other on the abaxial side. When almost dry, the nail-varnish imprints were peeled off
233 the leaf with the aid of a piece of transparent sticky tape. The tape was cut so as to keep the peeled
234 imprint and discard the rest. The imprint was transferred to a microscope slide and photographed
235 under a microscope (LEICA DMLB 2500, Germany). Two fields of view were selected from each
236 slide. There were no statistically significant differences among genotypes in the density of stomata
237 (Table SI2: abaxial, $p = 0.54$; adaxial, $p = 0.83$) were counted on images taken at $10\times$
238 magnification (the image size was $879 \mu\text{m} \times 659 \mu\text{m}$), or stomatal sizes (Table SI2: abaxial, $p =$
239 0.95 , adaxial, $p = 0.60$) measured in ImageJ on images at $20\times$ magnification (the image size was
240 $442 \mu\text{m} \times 331 \mu\text{m}$).

241 Optical properties of leaves

242 Leaf transmittance and absorptance was measured with a Jaz spectrometer from Ocean Optics
243 (Dunedin, USA) with four modules, DPU module, PX Pulsed Xenon Light source module and two
244 UV/VIS spectrometer modules, using a Spectroclip-TR probe consisting of two integrating spheres
245 facing each other on opposite sides of the leaf. A white/black reflectance target was used to obtain
246 a reference spectrum (Ocean Optics). The spectral reflectance and transmittance were both

247 measured at the same position on each of two leaves per plant, and used to estimate the spectral
248 absorptance (fraction of radiation absorbed expressed per nanometre was calculated as 1.0 minus
249 the sum of spectral reflectance and spectral transmittance). For each genotype, five replicates were
250 measured. We calculated the fraction of light absorbed by each genotype under RL, GL and BL
251 by multiplying the fractional spectral absorptance of the leaves by the light spectrum measured for
252 each LED channel (Aphalo 2015). The mean leaf absorptance was computed for each combination
253 of light channel and genotype based on the replicate estimates.

254 Data Analyses

255 Statistical analyses were done with R 3.2.0 (R Core Team 2016) within RStudio. Package mgcv
256 (Wood 2006) was used for fitting additive mixed models (AMM) and package nlme (Pinheiro and
257 Bates 2000) for fitting linear mixed effects (LME) models. The output of the R scripts used in the
258 analysis and both final and intermediate results are contained in a script (SI Script).

259 Because of the complex shape of the daily course of Δg_s we chose an additive model to test for
260 differences in the shape of the daily course among genotypes (Wood 2006). Additive models are
261 routinely used in various fields of research when data along the x -axis are densely spaced and
262 response-curve shapes are complex (e.g. de Dios *et al.* 2016 and Saw *et al.* 2017). An AMM was
263 fitted to Δg_s values with time-of-day as a continuous explanatory variable and genotype as a factor.
264 Each MT was compared with its corresponding WT. The AMM we fitted uses splines to describe
265 the change with time: it is a mixed model because it includes random terms and grouping factors
266 to describe the variability among plants. The model avoids pseudo-replication, as it takes each
267 plant as a replicate, even though 68 measured values were acquired from each plant. When
268 considering the shape of diurnal patterns of Δg_s in detail, our interpretation was based on
269 differences between the fitted curves and the overlap (or not) of the $p = 0.95$ confidence bands,
270 shown in the figures. Within each light treatment, overall differences between each MT and the
271 corresponding WT were assessed by formal, ANOVA-like tests of significance. A critical p value
272 of 0.05 for significance was used in these tests. We also used a more traditional approach fitting a
273 third-order polynomial (with an intercept forced to zero at ZT = 00:00 because of the use of Δg_s
274 values), in a linear mixed effects (LME) model, to analyse the time course during the first hour of
275 the photoperiod and confirm the validity of the AMM analysis.

276 A second-order polynomial was fitted to C_i/C_a and first-order polynomials to A_{net} and ΦPSII , using
277 LME models accounting for the repeated measures, as described above. Because of the steep
278 increase in A_{net} and ΦPSII and decrease in C_i/C_a immediately after the light was turned on at ZT =
279 00:00, which cannot be fitted to our LME models, data from the first cycle of measurements (ZT
280 = 00:00 to ZT = 00:30) were not included (SI Script).

281 **Results**

282 *Diurnal patterns of Δg_s and respiration in darkness*

283 Prior to the light treatments (ZT = 00:00), stomata were not completely closed in any genotype (g_s
284 $159 \pm 13 \text{ mmol m}^{-2} \text{ s}^{-1}$, mean \pm s.e. at ZT = 00:00). Nevertheless, during the last hour in the dark
285 (ZT = -01:00 to ZT = 00:00), Δg_s remained almost constant, increasing by less than 5 % in all
286 genotypes (SI Script).

287 In darkness, during what would otherwise be the normal photoperiod from ZT = 00:00 to ZT =
288 11:00, Δg_s in all genotypes slowly decreased as stomata continued to close from ZT = 00:00
289 onwards (Fig. 1a, b). The Δg_s of *phot1 phot2* was similar to its WT but in *cry1 cry2* Δg_s differed
290 from its WT by the end of the day. In *Ler* WT, Δg_s decreased by about $100 \text{ mmol m}^{-2} \text{ s}^{-1}$ during
291 the photoperiod but in *cry1 cry2* it only decreased approximately $60 \text{ mmol m}^{-2} \text{ s}^{-1}$ over the same
292 period (Fig. 1b).

293 In darkness, A_{net} was negative as a result of respiration, and was small in MTs and their respective
294 WTs (Fig. 1c, d). The slopes, describing the change in A_{net} with time, did not differ between *cry1*
295 *cry2* and its WT ($p = 0.90$; Fig. 1d), but did between *phot1 phot2* and its WT ($p < 0.0001$, Fig.
296 1c). The respiration rate in *phot1 phot2* decreased from the beginning to the end of the photoperiod
297 by $0.38 \mu\text{mol m}^{-2} \text{ s}^{-1}$ (respiration rate range: $1.63 - 1.25 \mu\text{mol m}^{-2} \text{ s}^{-1}$), whereas in its WT, this
298 decrease was only about $0.05 \mu\text{mol m}^{-2} \text{ s}^{-1}$ ($1.30 - 1.25 \mu\text{mol m}^{-2} \text{ s}^{-1}$) (Fig. 1c).

299 *Diurnal patterns of Δg_s under BL, GL and RL*

300 Fig. 2a shows the diurnal patterns of Δg_s under BL, GL and RL, as curves fitted using AMM and
301 their 95% confidence bands. In WTs, RL, GL and BL all induced stomatal opening at equal photon
302 irradiance of $200 \mu\text{mol m}^{-2} \text{ s}^{-1}$, but of these, BL was the most effective. Spectral measurements of
303 leaves and LEDs and calculations based on them showed that in-spite of differences in leaf

304 absorptance in the green-red region (516 - 643 nm) the estimated total absorbed flux of BL photons
305 was approximately 8% and 10% more than under RL or GL, respectively (Fig. SI6). Even though
306 the absorptance of leaves of *cry1 cry2* was slightly lower in the green-red region than that of the
307 other genotypes, the differences in absorbed photons between it and its *Ler* WT was 3% or less
308 under all light treatments (Fig. SI6a).

309 The maximum fitted Δg_s under BL was over $300 \text{ mmol m}^{-2} \text{ s}^{-1}$, approximately three times that
310 under GL or RL (Fig. 2). In *Ler* WT, Δg_s was higher in GL than in RL from ZT = 01:30 to ZT =
311 06:00. In addition to the differences in maximal Δg_s , the shape of the time course was different
312 under BL compared with GL or RL, in both *Ler* WT and Col-5 WT (Fig. 2a, b). The time courses
313 of g_s were consistent among replicate plants within treatments (Fig. SI3).

314 Under BL, the shapes of whole-day Δg_s time courses were strikingly different in the MTs compared
315 to their corresponding WTs (Fig. 2a, b). In the WTs, Δg_s increased rapidly upon illumination at
316 ZT = 00:00 and continued increasing, reaching $375 \text{ mmol m}^{-2} \text{ s}^{-1}$ (Col-5 WT) and 300 mmol m^{-2}
317 s^{-1} (*Ler* WT) at its maximum at ZT = 06:00 after which it started to decline. In the *phot1 phot2*
318 mutant (Col-5 background), Δg_s initially increased more gradually, reaching a maximum that was
319 only two thirds that of its WT, and later Δg_s decreased like in its WT (Fig. 2a, BL). In the *cry1 cry2*
320 mutant (*Ler* background), Δg_s was similar to that of its WT during the first 2 hours after the start
321 of illumination, but later in the day the maximum Δg_s in *cry1 cry2* was only approximately half
322 that of its WT, and likewise the decrease in Δg_s after ZT = 06:00 was smaller than in its WT (Fig.
323 2b, BL).

324 Under GL, the shape of the time course of Δg_s differed only between *cry1 cry2* and its WT and not
325 between *phot1 phot2* and its WT (Fig. 2a, b). During the first hour of illumination (ZT = 00:00 to
326 ZT = 01:00), Δg_s increased at a similar slow rate in all four genotypes (Fig. 5). From ZT = 02:00
327 to ZT = 06:00 Δg_s was 33% lower in *cry1 cry2* than in its WT (Fig. 2b).

328 Under RL, there were no significant differences in Δg_s between the MTs and their WTs and their
329 time courses had almost identical shapes (Fig. 2a, b). Plants of all four genotypes opened their
330 stomata slowly under RL, with Δg_s reaching approximately $90 \text{ mmol m}^{-2} \text{ s}^{-1}$ after one hour of
331 illumination (ZT = 01:00) and remaining at this relatively low value until ZT = 06:00, slowly
332 decreasing thereafter.

333 *Diurnal patterns of A_{net} under BL, GL and RL*

334 The diurnal time-courses of A_{net} , under BL, GL and RL are given in Fig. 2c and d, as curves fitted
335 using linear mixed effect models with 95% confidence bands. The first half hour of data (ZT =
336 00:00 to 00:30) were culled as the fast increase in A_{net} on illumination could not be adequately
337 captured by recordings at 20 min intervals. After the first half hour of the photoperiod in all light
338 treatments, A_{net} remained stable and no interaction between the three light treatments and
339 genotypes was detected ($p = 0.40$). A_{net} was highest under RL, lower under BL and lowest under
340 GL. The three-way interaction between time (change of A_{net} in time), light treatments and
341 genotypes was significant ($p < 0.0001$). Under BL, GL and RL, A_{net} was no higher in *Ler* WT than
342 in *Col-5* WT. In both WTs, A_{net} increased slowly during the photoperiod in all light treatments,
343 except under RL where in *Col-5* WT A_{net} remained almost constant ($p < 0.0001$). Under BL, A_{net}
344 in *phot1 phot2* tended to be lower than in its WT ($p = 0.074$), while the difference between *cry1*
345 *cry2* and its WT was not significant ($p = 0.63$). Under GL, over the day as a whole the MTs did
346 not differ from their respective WTs ($p \geq 0.10$). The slopes over the day of A_{net} differed statistically
347 between MTs and their respective WTs under BL, to a lesser extent GL (both $p < 0.001$), while
348 under RL their slopes were parallel ($p > 0.20$). In spite of their statistical significance relative rates
349 of change in A_{net} were small, ranging between $-1.5 \% h^{-1}$ and $+2 \% h^{-1}$ over treatments and
350 genotypes (Fig. 2c, d).

351 *Diurnal patterns of C_i/C_a under BL, GL, RL and in darkness*

352 The diurnal patterns of the ratio of intercellular carbon dioxide concentration to ambient carbon
353 dioxide concentration (C_i/C_a) as fitted second degree polynomials and 95% confidence bands are
354 given in Fig. 3. Data from ZT = 00:00 to 00:30 were not included for the same reason as for A_{net} .
355 There were no significant differences in C_i/C_a between genotypes under BL, GL, or RL ($p = 0.54$,
356 SI Script). However, for the photoperiod as a whole, the three-way interaction between light,
357 genotypes and time was significant ($p < 0.0001$, SI Script). The C_i/C_a ratio was lowest under RL,
358 highest in darkness, and similar in BL and GL. Under BL, the ratio initially increased and then
359 decreased from ZT = 06:00 onwards, in all genotypes except in *cry1 cry2* where it remained nearly
360 constant. The ratio of C_i/C_a under RL and GL was similar and slowly decreased towards the end
361 of the photoperiod. In darkness, the ratio was similar between MTs and their WT, slightly above
362 1.

363 *Diurnal patterns of Φ PSII under BL*

364 We investigated the diurnal patterns of Φ PSII under BL (Fig. 4a, b). Φ PSII in *phot1 phot2* was
365 lower than in its Col-5 WT ($p = 0.008$), decreasing from 16% lower at ZT = 00:30 to a maximum
366 difference of 22% at ZT = 10:00 (Fig 4a). In contrast, the Φ PSII in *cry1 cry2* was similar to its *Ler*
367 WT at ZT = 00:30, and differed by a maximum of only 13 % from *Ler* at ZT = 10:00 ($p = 0.016$,
368 Fig. 4b).

369 *Rate of increase in Δg_s at the start of illumination under BL, GL and RL*

370 Figure 5 shows fitted third order polynomials for Δg_s with 95% confidence bands for the first hour
371 (ZT = 00:00 to ZT = 01:00) under the light treatments. The model fitted to all the Δg_s data for this
372 period gave significant ($p < 0.001$, SI) two-way and three-way interactions between light colour,
373 genotype and time-of-day. This indicates that the differences between genotypes in the rate of
374 stomatal opening (slope of Δg_s against time) depended on the colour of the light to which the plants
375 were exposed. To identify these patterns, separate statistical analyses were done for each of the
376 light conditions: BL, GL and RL.

377 Under BL, Δg_s increased at a similar rate in both WTs ($p = 0.072$). While the rate of increase in
378 Δg_s did not differ between *cry1 cry2* and its WT ($p = 0.73$); in *phot1 phot2*, it was less than half
379 that of its WT ($p = 0.002$: Fig. 5). Under GL, there were no differences in Δg_s among the four
380 genotypes during the first hour of illumination ($p = 0.53$). However, under RL, Δg_s differed among
381 genotypes as the result of a slight difference in the shape of the time course during the first hour
382 of illumination in *phot1 phot2* compared to its WT ($p = 0.043$). Furthermore, under RL, the time
383 course of Δg_s was similar in both, *cry1 cry2* compared to its WT ($p = 0.15$), and between the two
384 WTs ($p = 0.15$).

385 In contrast to the illuminated plants, Δg_s of plants kept in darkness barely changed during the first
386 hour of what would have been the normal photoperiod. They followed the same time-course as
387 during the last hour before ZT = 00:00 with no clear differences between genotypes in the slope
388 of Δg_s against time ($p = 0.03$).

389 *Stomatal density and size*

390 Table 1 presents stomatal density and stomatal size for genotype *cry1 cry2*, its WT *Ler*, *phot1*
391 *phot2* and its WT Col-5. The slight differences observed between mutants and WTs were not
392 statistically significant (density: abaxial, $p = 0.54$; adaxial, $p = 0.83$; size: abaxial, $p = 0.95$, adaxial,
393 $p = 0.60$, Tab. 1).

394 **Discussion**

395 For half a century, diurnal patterns in g_s have been described using gas-exchange methods (e.g.
396 Tenhunen *et al.* 1987). More recently the use of photoreceptor mutants has improved our
397 understanding of the mechanisms behind stomatal responses to light (e.g. Boccacandro *et al.* 2012).
398 Here, we combined these two approaches to investigate the roles of *crys* and *phots* in stomatal
399 opening throughout the day.

400 *The control of diurnal patterns in g_s and A_{net} under BL, GL and RL*

401 Parallel changes in g_s and A_{net} over the diurnal period are ubiquitous because A_{net} depends on CO₂
402 entering the leaf through stomata. Cowan and Farquhar (1977) were first to consider the theoretical
403 question of what would be the day course of g_s that minimises daily water loss relative to a given
404 level of whole-day carbon assimilation, proposing a model based on an optimization criterion.
405 However, actual measurements of g_s through the day frequently deviate from the predictions of
406 Cowan and Farquhar's (1977) model (Matthews *et al.* 2017).

407 Regulation of fluxes of CO₂ and water vapour by stomata depends both on functional coupling
408 between g_s and A_{net} and on independent regulation of g_s and A_{net} through parallel responses to the
409 same, or correlated, stimuli (Zeiger *et al.* 1982; Aphalo and Sánchez 1986; Aphalo and Jarvis
410 1993). Under all three of our 11-h constant irradiance treatments (BL, GL, RL), we observed clear
411 diurnal changes in g_s (Figs. 2a, b), while Φ_{PSII} and A_{net} concurrently varied much less (Fig. 2c, d;
412 Fig. 4), which indicates that functional dependence of g_s on A_{net} is unable to fully explain our
413 results. Differences in responses to light of different colours can inform us about the relative
414 importance of functional coupling between g_s and A_{net} vs. direct stomatal responses to light
415 (Mansfield and Meidner 1966; Aphalo and Sánchez 1986).

416 Faster stomatal opening at the beginning of the photoperiod under BL than under RL (Fig. 5) is
417 consistent with the rapid stomatal opening commonly seen in response to acute BL treatments
418 (reviewed by Shimazaki *et al.* 2007). Such direct induction of BL-specific stomatal opening can
419 happen almost immediately, often within seconds of illumination (Zeiger *et al.* 1987; Lawson *et*
420 *al.* 2010).

421 The larger Δg_s under BL than under RL throughout the diurnal time-course irrespective of the
422 lower A_{net} and higher C_i (Fig. 2), which might otherwise be expected to negatively regulate Δg_s ,
423 indicates that BL-specific maintenance of stomatal opening was active during the whole
424 photoperiod. These results are similar to the gas-exchange time-courses observed in *Xanthium*
425 *strumarium* by Sharley and Raschke (1981) under BL (peak $\lambda = 455$ nm) and RL ($\lambda = 681$ nm,
426 applied for 4 h). In this earlier experiment combined RL and BL at $650 \mu\text{mol m}^{-2} \text{s}^{-1}$ photon
427 irradiance gave g_s of $300 \text{ mmol m}^{-2} \text{s}^{-1}$ after 1 h; g_s remained high at $250 \text{ mmol m}^{-2} \text{s}^{-1}$ under BL
428 alone, while just RL gave a g_s of only $60 \text{ mmol m}^{-2} \text{s}^{-1}$. Given the lower C_i under RL than under
429 BL, the moderately larger Δg_s under RL compared to darkness over the photoperiod could be
430 explained, at least in part, by feedback control on stomatal opening through coupling mediated by
431 C_i depletion.

432 To a lesser extent than under BL, under GL higher g_s and C_i and lower A_{net} than under RL were
433 maintained throughout the diurnal period, suggesting a contribution from photoreceptors to
434 stomatal opening in GL. Such a role for photoreceptors in GL is consistent with Wang *et al.*'s
435 (2011) observation of A_{net} -independent components in stomatal responses under both BL and GL
436 in sunflower treated with DCMU. Taken together, the different responses we observed under BL,
437 GL and RL indicate that the increase in Δg_s on illumination, and its maintenance throughout the
438 diurnal period, under both BL and GL may partly depend on the BL photoreceptors (discussed
439 next).

440 *The roles of crys and phots in stomatal opening at the start of the day and throughout the*
441 *photoperiod*

442 The leaf traits of photoreceptor-mutant plants can differ from those of their WT, irrespective of
443 light treatments (Labuz *et al.* 2012; Yu *et al.* 2010). Differences in leaf anatomy, such as in
444 stomatal size and density, can result from the participation of crys in stomatal development (Li

445 and Yang 2007; Boccalandro *et al.* 2012). However, we found no significant differences between
446 *cry1 cry2* and its *Ler* WT in stomatal size or density (Table SI2), which might otherwise have
447 confounded the response of g_s attributable to *crys*. Differences in light absorptance are dependent
448 on concentration per unit area of chlorophyll and other pigments in leaves which might be
449 modulated through the action of photoreceptors (Hogewoning *et al.* 2010; Thum *et al.* 2001), but
450 these differences were small compared to the responses of Δg_s and A_{net} in our experiment. Likewise,
451 recordings of g_s before the light treatments and in the darkness treatment (Fig. 1a, b) detected no
452 constitutive differences between the MTs and their respective WTs. Nevertheless, different
453 interactions among photoreceptors are likely to affect responses to full-spectrum solar radiation
454 compared to the monochromatic BL-, RL- and GL treatments employed in our experiments.

455 The most striking feature differentiating the response of the genotypes under BL was the difference
456 in rate of stomatal opening on illumination (Fig. 5). The rapid stomatal response upon BL
457 illumination we observed in WTs concurs with the findings of Kinoshita *et al.* (2001) that rapid
458 membrane depolarization follows BL illumination (within 30s), which implies that communication
459 between nucleus and plasma membrane is too rapid to implicate changes in gene expression in this
460 response (Shimazaki *et al.* 2007). The lack of a rapid response to BL in the *phot1 phot2* MT agrees
461 with the accepted view for the key role of *phots* in stomatal opening from experiments of shorter
462 duration than ours (Shimazaki *et al.* 2007). After 2 h 30 min under BL, g_s of *phot1 phot2* was about
463 50% less than that of its WT Col-5 (ZT > 02:30, Fig. 2a, b), indicating that *phots* continue to
464 contribute to maintaining g_s after the rapid initial opening. This result concurs with the role of
465 *phots* in the promotion of continuous stomatal opening through the diurnal period under full
466 sunlight (Boccalandro *et al.* 2012).

467 Previous studies report that *crys* can contribute to blue-light-induced stomatal opening under low
468 irradiances ($< 100 \mu\text{mol s}^{-1} \text{m}^{-2}$, Mao *et al.* 2005). However, Boccalandro *et al.* (2012) found *crys*
469 not to be directly involved in the perception of those signals that promote BL-specific stomatal
470 opening in an experiment under solar radiation (full spectrum). They found that under full sunlight
471 the diurnal patterns of g_s in *cry1 cry2* and *phot1 phot2* had similar shapes to those of their WT, but
472 that *phot1 phot2* had much lower g_s , though both photoreceptors enhanced A_{net} . Our results showed
473 a specific role for *crys* under BL in the promotion of stomatal opening: following rapid stomatal
474 opening induced by *phots*, *crys* were needed for the maintenance of high Δg_s from 2 h 30 min

475 through the remainder of the photoperiod (ZT > 02:30, Fig. 2a, b). In contrast, A_{net} was comparable
476 in *cry1 cry2* and its WT but C_i was lower in the MT (Figs. 2 and 3), indicating a contribution of
477 *crys* to stomatal opening mainly independent of A_{net} . It can be speculated that stomatal responses
478 mediated by *crys* are slower than those mediated by *phots* because *crys*' action usually depends on
479 regulation of gene expression (Ohgishi *et al.* 2004).

480 Interestingly, adding together Δg for the two MTs at each time point throughout the diurnal cycles
481 under BL yields a similar pattern of Δg to that observed in the WTs. This might be interpreted as
482 evidence for an additive effect of *phot* and *cry* after 2 h 30 min. This is consistent with Mao *et al.*'s
483 (2005) finding that stomatal aperture in a quadruple MT *cry1 cry2 phot1 phot2* measured on
484 epidermal strips was reduced under $20 \mu\text{mol s}^{-1} \text{m}^{-2}$ BL, compared to that in either of the double
485 MTs *cry1 cry2* or *phot1 phot2*. Further research is needed to better explain how these
486 photoreceptors interact and function together in the control of stomatal opening through the whole
487 diurnal period.

488 In our experiment, Δg_s was larger under GL than under RL, agreeing with a few reports of stomatal
489 opening driven by GL (Smith *et al.* 2017). Earlier studies did not investigate the involvement of
490 specific photoreceptors in opening of stomata in GL. Consistently with the weak absorption of GL
491 by *phots* (Christie *et al.* 2015), we found no evidence for a role of *phots* in stomatal opening in GL.
492 In contrast, Δg_s under GL was smaller in *cry1 cry2* than in its WT (Fig. 2b), with *crys* accounting
493 for up to 35% of Δg_s 3 h into the photoperiod, indicating a role for them in stomatal opening under
494 GL. This role is consistent with other *cry*-dependent GL responses and the absorption of GL by
495 light-adapted *crys* (Folta and Maruhnich 2007; Banerjee *et al.* 2007).

496 Evidence for *crys*' involvement in responses of stomata to BL (such as Mao *et al.* 2005 and the
497 present study), and in other responses to GL such as shade avoidance (Sellaro *et al.* 2010), de-
498 etiolation (Lin *et al.* 1995) and inhibition of hypocotyl elongation (Ahmad *et al.* 2002), are also
499 consistent with a role for *crys* in stomatal opening in monochromatic GL. While it has been also
500 observed that GL (540 nm) can antagonise BL-induced stomatal opening (Talbot *et al.* 2002),
501 which is an effect that has been attributed to NPQ1 instead of *phots* or *crys* (Talbot *et al.* 2003),
502 our results suggest a positive effect of GL at 516 nm on stomatal opening mediated by *crys*.

503 The diurnal course of gas-exchange differs among species (Matthews *et al.* 2017). The differences

504 are in the speed of stomatal opening at the start of photoperiod and in the later slower increase or
505 decrease in g_s through the rest of the day. Fast opening is important for timely increase in g_s in the
506 morning and in sun flecks (Zeiger *et al.* 1981), improving light utilization for carbon assimilation
507 (Way and Pearcy 2012). Within species, acclimation to different light environments can result in
508 different stomatal opening speeds on exposure to light (Aasamaa and Aphalo 2017; Way and
509 Pearcy 2012). This suggests that separate regulation of opening speed and g_s steady state is possible.
510 The fast phot-dependent response together with the slower cry-dependent BL-specific response
511 could allow such separate regulation of the opening speed and g_s steady-state, providing additional
512 flexibility in the coordination of g_s and A_{net} . As the combined roles of phots and crys in stomatal
513 opening are likely to depend on plants' native habitat and growing conditions, their study will
514 require measurements of whole-day time courses under realistic manipulations and/or simulations
515 of the natural light environment.

516 **Conclusions**

517 We conclude that under an 11 h photoperiod with constant irradiance of $200 \mu\text{mol m}^{-2} \text{s}^{-1}$: (1)
518 monochromatic BL induces a diurnal pattern of g_s with a broad maximum near ZT = 6:00 to ZT =
519 7:00 that is different to that under RL or GL; (2) the normal diurnal pattern of g_s in BL requires
520 phots for rapid stomatal opening at the beginning of the photoperiod and both phots and crys
521 afterwards; (3) stomatal opening in GL at 516 nm does not require phots but is likely to partly
522 depend on crys.

523 **Acknowledgments**

524 This research was made possible by funding from the Academy of Finland (decisions 252548 to
525 PJA, and 324555 and 304519 to TMR), China Scholarship Council, The Ella and Georg Ehrnrooth
526 Foundation and Niemi Foundation (to FW). We also thank Dr. Mikael Brosché (University of
527 Helsinki) for seeds of the *cry1 cry2* Arabidopsis mutant.

528 **Conflict of Interest Statement**

529 The authors declare no conflicts of interest

530

531 **References**

- 532 Ahmad M, Grancher N, Heil M, Black RC, Giovani B, Galland P, Lardemer D (2002) Action
533 spectrum for cryptochrome-dependent hypocotyl growth inhibition in Arabidopsis. *Plant*
534 *Physiology* **129**, 774–785.
- 535 Ando E, Ohnishi M, Wang Y, Matsushita T, Watanabe A, Hayashi Y, Fujii M, Ma JF, Inoue S-I,
536 Kinoshita T (2013) TWIN SISTER OF FT, GIGANTEA, and CONSTANS have a positive
537 but indirect effect on blue light-induced stomatal opening in Arabidopsis. *Plant Physiology*
538 **162**, 1529–1538.
- 539 Aphalo PJ (2015) The r4photobiology suite: spectral irradiance. *UV4Plants Bulletin* **2015**, 21–
540 29.
- 541 Aphalo PJ, Jarvis PG (1993) Separation of Direct and Indirect Responses of Stomata to Light -
542 Results From a Leaf Inversion Experiment at Constant Intercellular CO₂ Molar Fraction.
543 *Journal of experimental botany* **44**,791–800.
- 544 Aphalo PJ, Sánchez RA (1986) Stomatal Responses to Light and Drought Stress in Variegated
545 Leaves of *Hedera helix*. *Plant Physiology* **81**,768–773
- 546 Aasamaa K, Aphalo PJ (2017) The acclimation of *Tilia cordata* stomatal opening in response to
547 light, and stomatal anatomy to vegetational shade and its components. *Tree Physiology* **37**,
548 209–219
- 549 Banerjee R, Batschauer A (2005) Plant blue-light receptors. *Planta* **220**, 498–502.
- 550 Banerjee R, Schleicher E, Meier S, Viana RM (2007) The signaling state of Arabidopsis
551 cryptochrome 2 contains flavin semiquinone. *Journal of Biological Chemistry* **282**,14916–
552 14922.
- 553 Bocalandro HE, Giordano CV, Ploschuk EL, Piccoli PN, Bottini R, Casal JJ (2012)
554 Phototropins But Not Cryptochromes Mediate the Blue Light-Specific Promotion of
555 Stomatal Conductance, While Both Enhance Photosynthesis and Transpiration under Full
556 Sunlight. *Plant Physiology* **158**, 1475–1484.

- 557 Briggs WR, Huala E (1999) Blue-light photoreceptors in higher plants. *Annual review of cell and*
558 *developmental biology* **15**, 33–62.
- 559 Chen C, Xiao Y, Li X, Ni M (2012) Light-Regulated Stomatal Aperture in Arabidopsis.
560 *Molecular plant* **5**, 566–572.
- 561 Christie JM (2007) Phototropin blue-light receptors. *Annual Review of Plant Biology* **58**, 21–45.
- 562 Christie JM, Blackwood L, Petersen J, Sullivan S (2015) Plant flavoprotein photoreceptors. *Plant*
563 *and Cell Physiology* **56**, 401–413.
- 564 Cowan IR, Farquhar GD (1977) Stomatal function in relation to leaf metabolism and
565 environment. *Symposia of the Society for Experimental Biology* **31**, 471–505.
- 566 de Dios VR, Gessler A, Ferrio JP, Alday JG, Bahn M, del Castillo J, Devidal S, García-Muñoz S,
567 Kayler Z, Landais D, Martín-Gómez P, Milcu A, Piel C, Pirhofer-Walzl K, Ravel O, Salekin
568 S, Tissue DT, Tjoelker MG, Voltas J, Roy J (2016) Circadian rhythms have significant
569 effects on leaf-to-canopy scale gas exchange under field conditions. *GigaScience* **5**, 1-10
- 570 Inoue S-I, Takemiya A, Shimazaki K-I (2010) Phototropin signaling and stomatal opening as a
571 model case. *Current Opinion in Plant Biology* **13**, 587–593.
- 572 Folta KM, Maruhnich SA (2007) Green light: a signal to slow down or stop. *Journal of*
573 *experimental botany* **58**, 3099–3111.
- 574 Frechilla S, Talbott LD, Bogomolni RA, Zeiger E (2000) Reversal of Blue Light-Stimulated
575 Stomatal Opening by Green Light. *Plant and Cell Physiology* **41**, 171–176.
- 576 Genty B, Briantais J-M, Baker NR (1989) The relationship between the quantum yield of
577 photosynthetic electron transport and quenching of chlorophyll fluorescence. *Biochimica Et*
578 *Biophysica Acta (BBA) - General Subjects* **990**, 87–92.
- 579 Hogewoning SW, Trouwborst G, Maljaars H, POORTER H, van Ieperen W, Harbinson J (2010)
580 Blue light dose-responses of leaf photosynthesis, morphology, and chemical composition of
581 *Cucumis sativus* grown under different combinations of red and blue light. *Journal of*

582 *Experimental Botany* **61**, 3107–3117.

583 Kinoshita T, Doi M, Suetsugu N, Kagawa T, Wada M, Shimazaki K (2001) Phot1 and phot2
584 mediate blue light regulation of stomatal opening. *Nature* **414**, 656–660.

585 Kinoshita T, Ono N, Hayashi Y, Morimoto S, Nakamura S, Soda M, Kato Y, Ohnishi M, Nakano
586 T, Inoue S-I, Shimazaki K-I (2011) FLOWERING LOCUS T Regulates Stomatal Opening.
587 *Current Biology* **21**, 1232–1238.

588 Labuz J, Sztatelman O, Banas AK, Gabrys H (2012) The expression of phototropins in
589 Arabidopsis leaves: developmental and light regulation. *Journal of Experimental Botany* **63**,
590 1763–1771.

591 Lawson T, Caemmerer von S, Baroli I (2010) Photosynthesis and Stomatal Behaviour. pp. 265–
592 304 in *Progress in Botany Springer Berlin Heidelberg*: Berlin, Heidelberg.

593 Li Q-H, Yang H-Q (2007) Cryptochrome signaling in plants. *Photochemistry and Photobiology*
594 **83**, 94–101.

595 Lin C, Ahmad M, Gordon D, Cashmore AR (1995) Expression of an Arabidopsis cryptochrome
596 gene in transgenic tobacco results in hypersensitivity to blue, UV-A, and green light.
597 *Proceedings of the National Academy of Sciences* **92**, 8423–8427.

598 Liscum E, Hodgson DW, Campbell TJ (2003) Blue light signaling through the cryptochromes
599 and phototropins. So that's what the blues is all about. *Plant Physiology* **133**, 1429–1436.

600 Mao J, Zhang Y-C, Sang Y, Li Q-H, Yang H-Q (2005) From The Cover: A role for Arabidopsis
601 cryptochromes and COP1 in the regulation of stomatal opening. *Proceedings of the National*
602 *Academy of Sciences* **102**, 12270–12275.

603 Matthews JSA, Vialet-Chabrand SRM, Lawson T (2017) Diurnal Variation in Gas Exchange:
604 The Balance between Carbon Fixation and Water Loss. *Plant Physiology* **174**, 614–623

605 Ohgishi M, Saji K, Okada K, Sakai T (2004) Functional analysis of each blue light receptor,
606 cry1, cry2, phot1, and phot2, by using combinatorial multiple mutants in Arabidopsis.

607 *Proceedings of the National Academy of Sciences* **101**, 2223–2228.

608 Pinheiro JC, Bates DM (2000) Nonlinear Mixed-Effects Models: Basic Concepts and Motivating
609 Examples pp. 273–304 in *Mixed-Effects Models in Sand S-PLUS*. Statistics and Computing.
610 Springer New York: New York, NY.

611 R Core Team (2016) R: A Language and Environment for Statistical Computing. Vienna,
612 Austria.

613 Roelfsema MRG, Hanstein S, Felle HH, Hedrich R (2002) CO₂ provides an intermediate link in
614 the red light response of guard cells. *The Plant Journal* **32**, 65–75.

615 Saw NMMT, Moser C, Martens S, Franceschi P (2017) Applying generalized additive models to
616 unravel dynamic changes in anthocyanin biosynthesis in methyl jasmonate elicited grapevine
617 (*Vitis vinifera* cv. Gamay) cell cultures. *Horticulture Research* **4**, 17038.

618 Sellaro R, Crepy M, Trupkin SA, Karayekov E, Buchovsky AS, Rossi C, Casal JJ (2010)
619 Cryptochrome as a sensor of the blue/green ratio of natural radiation in Arabidopsis. *Plant*
620 *Physiology* **154**, 401–409.

621 Sellaro R, Pacín M, Casal JJ (2012) Diurnal dependence of growth responses to shade in
622 Arabidopsis: role of hormone, clock, and light signaling. *Molecular plant* **5**, 619–628.

623 Sharkey TD, Raschke K (1981) Effect of Light Quality on Stomatal Opening in Leaves of
624 *Xanthium strumarium* L. *Plant Physiology* **68**, 1170–1174.

625 Sharkey TD, Ogawa T (1987) Stomatal responses to light pp. 195-208 in *Stomatal function*. (ed.
626 Zeiger E, Farquhar GD, Cowan IR) Stanford University Press

627 Shimazaki K-I, Doi M, Assmann SM, Kinoshita T (2007) Light Regulation of Stomatal
628 Movement. *Annual Review of Plant Biology* **58**, 219–247.

629 Smith HL, McAusland L, Murchie EH (2017) Don't ignore the green light: exploring diverse
630 roles in plant processes. *Journal of experimental botany* **68**, 2099–2110.

631 Talbott LD, Zeiger E (1996) Central Roles for Potassium and Sucrose in Guard-Cell

632 Osmoregulation. *Plant Physiology* **111**, 1051–1057.

633 Talbott LD, Nikolova G, Ortiz A, Shmayevich I, Zeiger E (2002) Green light reversal of blue-
634 light-stimulated stomatal opening is found in a diversity of plant species. *American Journal*
635 *of Botany* **89**, 366–368.

636 Talbott LD, Shmayevich IJ, Chung Y, Hammad JW, Zeiger E (2003) Blue light and
637 phytochrome-mediated stomatal opening in the *npq1* and *phot1 phot2* mutants of
638 *Arabidopsis*. *Plant Physiology* **133**, 1522–1529.

639 Tallman G (2004) Are diurnal patterns of stomatal movement the result of alternating
640 metabolism of endogenous guard cell ABA and accumulation of ABA delivered to the
641 apoplast around guard cells by transpiration? *Journal of experimental botany* **55**, 1963–1976.

642 Tenhunen JD, Pearcy RW, Lange OL (1987) Diurnal Variations in Leaf Conductance and Gas
643 Exchange in Natural Environments. (eds. E Zeiger, GD Farquhar and IR Cowan) *Stomatal*
644 *function*. Stanford University Press, 323-351

645 Thum KE, Kim M, Christopher DA, Mullet JE (2001) Cryptochrome 1, cryptochrome 2, and
646 phytochrome a co-activate the chloroplast *psbD* blue light-responsive promoter. *The Plant*
647 *Cell Online* **13**, 2747–2760.

648 Yu X, Liu H, Klejnot J, Lin C (2010) The Cryptochrome Blue Light Receptors. *The Arabidopsis*
649 *Book* **8**, e0135.

650 Wang F (2017) Tutorial: SIOX plugin in ImageJ: area measurement made easy. *UVPlants*
651 *Bulletin* **2**.

652 Wang Y, Noguchi K, Terashima I (2011) Photosynthesis-dependent and -independent responses
653 of stomata to blue, red and green monochromatic light: differences between the normally
654 oriented and inverted leaves of sunflower. *Plant and Cell Physiology* **52**, 479–489.

655 Way DA, Pearcy RW (2012) Sunflecks in trees and forests: from photosynthetic physiology to
656 global change biology. *Tree Physiology* **32**, 1066–1081.

- 657 Wood S (2006) *Generalized Additive Models: an introduction with R*. CRC Press
- 658 Zeiger E, Field C (1982) Photocontrol of the Functional Coupling between Photosynthesis and
659 Stomatal Conductance in the Intact Leaf : Blue Light and Par-Dependent Photosystems in
660 Guard Cells. *Plant Physiology* **70**, 370–375.
- 661 Zeiger E, Field C, Mooney HA (1981) Stomatal opening at dawn: possible roles of the blue light
662 response in nature in *Plants and the Daylight Spectrum*. Academic Press. 391-407
- 663 Zeiger E, Iino M, Shimazaki K-I, Ogawa T (1987) The blue-light response of stomata. In
664 Stomatal function. Stanford University Press. 209-227
- 665

666 **Figure legends**

667 Fig. 1. Time courses of gas-exchange between ZT = 00:00 and ZT = 11:30 in darkness in *phot1*
668 *phot2* (---), its WT Col-5 (—), *cry1 cry2* (---) and its WT *Ler* (—). (a, b) Change in stomatal
669 conductance (Δg_s) from ZT = 00:00; (c, d) Net carbon assimilation rate (A_{net}). Negative net
670 carbon assimilation rate in darkness is respiration. Lines depict prediction by a fitted additive
671 mixed models (AMM) (a, b) and mixed-effect linear models (c, d); grey bands depict 95%
672 confidence limits; n = 3 – 4 plants per genotype, N = 14 plants, 1040 observations in total. The
673 vertical dashed lines highlight ZT = 00:00, the time when LEDs were switched on during gas-
674 exchange measurements for treatments not remaining in darkness.

675 Fig. 2 Time courses of gas-exchange between ZT = 00:00 and ZT = 11:30 under constant
676 irradiance of BL, GL, or RL in *phot1 phot2* (---), its WT Col-5 (—), *cry1 cry2* (---) and its WT
677 *Ler* (—). (a, b) Change in stomatal conductance (Δg_s) from ZT = 00:00; (c, d) Net carbon
678 assimilation rate (A_{net}). Lines depict prediction by a fitted additive mixed models (AMM) (a, b)
679 and mixed effects model based on mixed-effect linear models (c, d) ; grey bands depict 95%
680 confidence limits; n = 3 – 4 plants per light colour and genotype, N = 44 plants, 3371
681 observations in total. The vertical dashed lines highlight ZT = 00:00, the time when LEDs were
682 switched on during gas-exchange measurements, except for plants remaining in darkness.
683 Equivalent figures showing raw g_s and A_{net} data are presented in Figs. SI 4 and 5 respectively.

684 Fig. 3 Ratio of intercellular and ambient carbon dioxide (C_i/C_a) in *phot1 phot2* (---) and its WT
685 Col-5 (—) under constant irradiance of BL (a), GL (b), RL (c) and in darkness (d), and in *cry1*
686 *cry2* (---) and its WT *Ler* (—) under BL (e), GL (f), RL (g) and in darkness (h) between ZT =
687 00:30 and ZT = 11:30. Lines depict prediction by a fitted mixed effects model based on linear
688 models and grey bands depict 95% confidence limits, n = 3 – 4 plants per light colour and
689 genotype, N = 44 plants, 4262 observations in total. The vertical dashed lines highlight ZT =
690 00:00, the time when LEDs were switched on during gas-exchange measurements, except for
691 plants remaining in darkness. The C_a is given in Table SII.

692 Fig. 4 Effective photochemical quantum yield of photosystem PSII photochemistry (Φ_{PSII})
693 under constant irradiance of BL between ZT = 00:30 and ZT = 11:30 in *phot1 phot2* (---) and its
694 WT Col-5 (—) (a) and in *cry1 cry2* (---) and its WT *Ler* (—) (b). Lines depict prediction by a
695 fitted mixed effects model based on linear models and grey bands depict 95% confidence limits,

696 n = 4 plants per light colour and genotype, N = 62 plants, 3828 observations in total. The vertical
697 dashed lines highlight ZT = 00:00, the time when LEDs were switched on during gas-exchange
698 measurements, except for plants remaining in darkness.

699 Fig. 5 Change in stomatal conductance (Δg_s) in *phot1 phot2* (---) and its WT Col-5 (—) under
700 constant irradiance of BL (a), GL (b), RL (c) and in darkness (d), and in *cry1 cry2* (---) and its
701 WT *Ler* (—) under BL (e), GL (f), RL (g) and in darkness (h) between ZT = 00:00 and ZT =
702 01:00. Lines depict prediction by a fitted mixed effects model based on third-order polynomials
703 and grey bands depict 95% confidence limits, n = 3 – 4 plants per light colour and genotype, N =
704 58 plants, 340 observations in total. Data of g_s for individual plants are given in Fig. SI4. The
705 vertical dashed lines highlight ZT = 00:00, the time when LEDs were switched on during gas-
706 exchange measurements, except for plants remaining in darkness

707 **Legends to supplemental figures**

708 Fig. SI1 Spectral photon irradiance measured in the growth room with a cosine diffuser level
709 with the top of the seedlings. Spectral irradiance on the growth room shelves was measured with
710 a Maya2000 Pro spectrometer (Ocean Optics, U.S.A) fitted with a D7-H-SMA cosine diffuser
711 (Bentham Instruments, Reading, U.K.).

712 Fig. SI2a Normalized spectral photon irradiance of (non-polarized) light emitted by the red,
713 green, and blue channels of the LED-array source used for gas-exchange measurements
714 (presented in Fig SI3, SI4 and SI5). The overlap in normalized photon irradiance between the
715 blue and green channels is 3.9% of their combined photon irradiance, and between green and red
716 channels the overlap is 0.4%. There is no measurable overlap (<0.05%) between red and blue
717 channels; SI2b Photograph of the custom-built LED-array light source used for gas-exchange
718 measurements. Each array has three independent channels, emitting BL, GL, or RL.

719 Fig. SI3 Stomatal conductance (g_s) for individual plants from 12 midnight until 6 p.m. on the
720 next day. These data were used to calculate the Δg_s values used in the model fits presented in
721 Figs. 2 and 3, and in statistical tests of significance. The vertical dashed lines highlight 7 a.m.
722 local time (ZT = 00:00), the time when LEDs were switched on during gas-exchange
723 measurements, except for plants remaining in darkness.

724 Fig. SI4 Net carbon assimilation rate (A_{net}) for individual plants from 12 midnight until 6 p.m. on
725 the next day. These data were used to calculate A_{net} values used in the model fits presented in
726 Figs. 2 and 3, and in statistical tests of significance. Negative net carbon assimilation rate in
727 darkness is respiration. The vertical dashed lines highlight 7 a.m. local time (ZT = 00:00), the
728 time when LEDs were switched on during gas-exchange measurements, except for plants
729 remaining in darkness.

730 Fig. SI5 Ratio of C_i/C_a for individual plants from 12 midnight until 6 p.m. on the next day. These
731 data were used to calculate ratio of C_i/C_a values used in the model fits presented in Figs. 4, and in
732 statistical tests of significance. The vertical dashed lines highlight 7 a.m. local time (ZT = 00:00),
733 the time when LEDs were switched on during gas-exchange measurements, except for plants
734 remaining in darkness. Concentrations of C_a are listed in Table SI1.

735 Fig. SI6 Light absorption. Average spectral absorptance of illuminated leaves from 5 or 6 plants
736 of each genotype. Upper panel: The colour bars show the full width at half maximum (FWHM)
737 of the peak of photon emission spectra of the three LED channels from Fig. SI2a. Lower panel:
738 Estimate of the photon dose rate computed as the absorbed irradiance by convolution of the
739 absorptance spectra of the leaves (upper panel) with the emission spectra of the LEDs (Fig. SI2a)
740 integrated over wavelengths. The dashed line indicates the photon irradiance incident on the
741 plants. The absorbed energy irradiances averaged over genotypes were: RL 34.3 W m^{-2} , GL 41.4
742 W m^{-2} , and BL 50.4 W m^{-2} .

743

744

745 **Tables**

746 **Table 1.** Stomatal size and density, mean \pm SE, n = 10. Size is expressed as the maximum length
 747 of the guard cells along the length of the pore; density is expressed as number of stomata per unit
 748 leaf area.

Genotype	Epidermis	Size (μm)	Density (mm^{-2})
Col-5	Adaxial	18.6 \pm 0.4	163 \pm 11
	Abaxial	19.2 \pm 1.4	191 \pm 16
<i>phot1 phot2</i>	Adaxial	18.6 \pm 0.4	142 \pm 32
	Abaxial	19.2 \pm 1.4	184 \pm 28
Ler	Adaxial	20.3 \pm 0.8	164 \pm 27
	Abaxial	19.0 \pm 1.0	171 \pm 17
<i>cry1 cry2</i>	Adaxial	18.8 \pm 0.5	150 \pm 17
	Abaxial	19.0 \pm 1.0	146 \pm 18

749

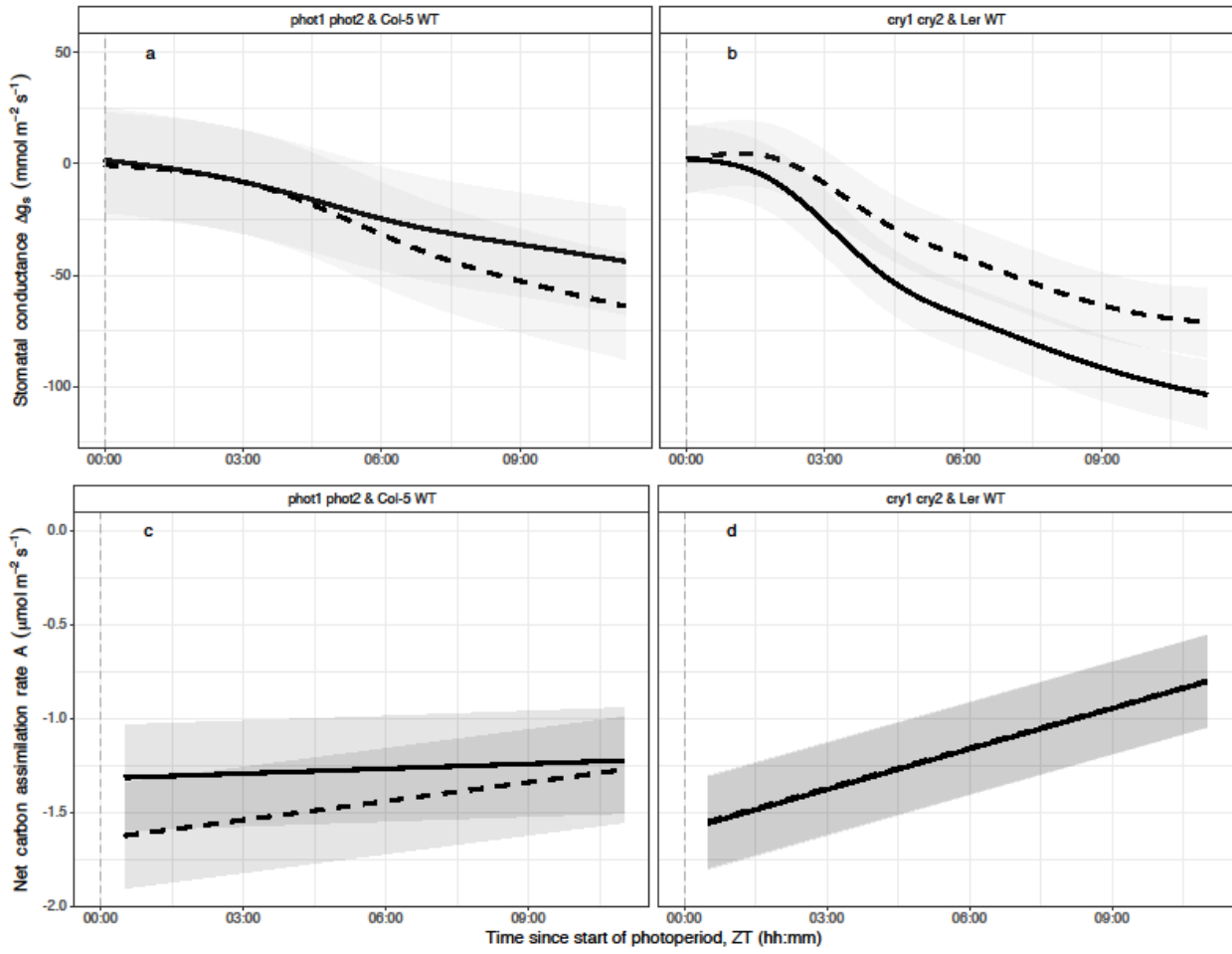
750 **Table SII.** Concentration of C_a maintained by gas-exchange system under each light treatment
 751 for each genotype during the period of ZT = 00:00 to ZT = 11:30.

	Red light	Green light	Blue light	Darkness
Col-5	387.6 \pm 0.1	387.8 \pm 0.1	387.6 \pm 0.1	390.3 \pm 0.0
<i>phot1 phot2</i>	388.4 \pm 0.0	388.1 \pm 0.1	388.4 \pm 0.1	390.3 \pm 0.0
Ler	386.9 \pm 0.1	387.4 \pm 0.1	386.9 \pm 0.1	390.1 \pm 0.0
<i>cry1 cry2</i>	387.8 \pm 0.1	387.9 \pm 0.1	387.8 \pm 0.1	390.1 \pm 0.0

752

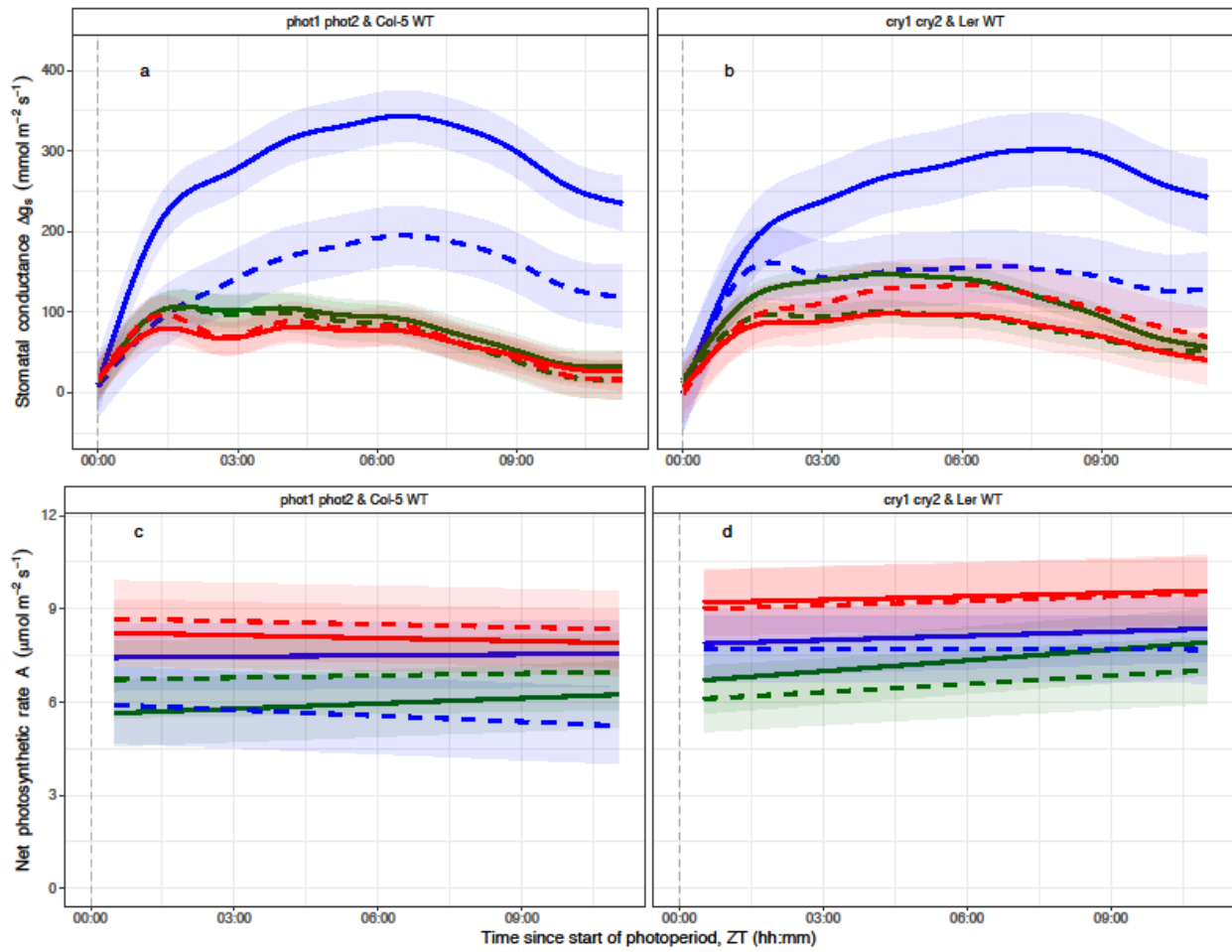
753

754 Fig. 1



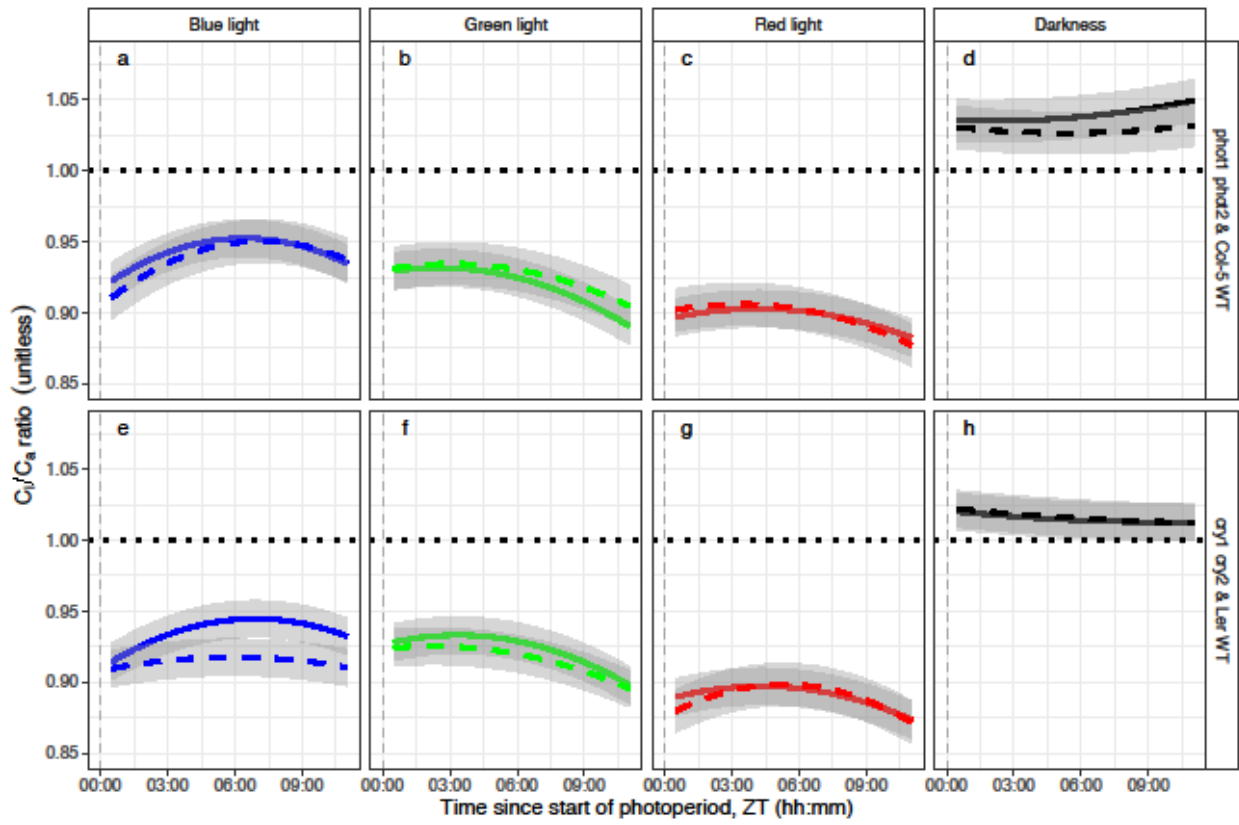
755

756 Fig. 2



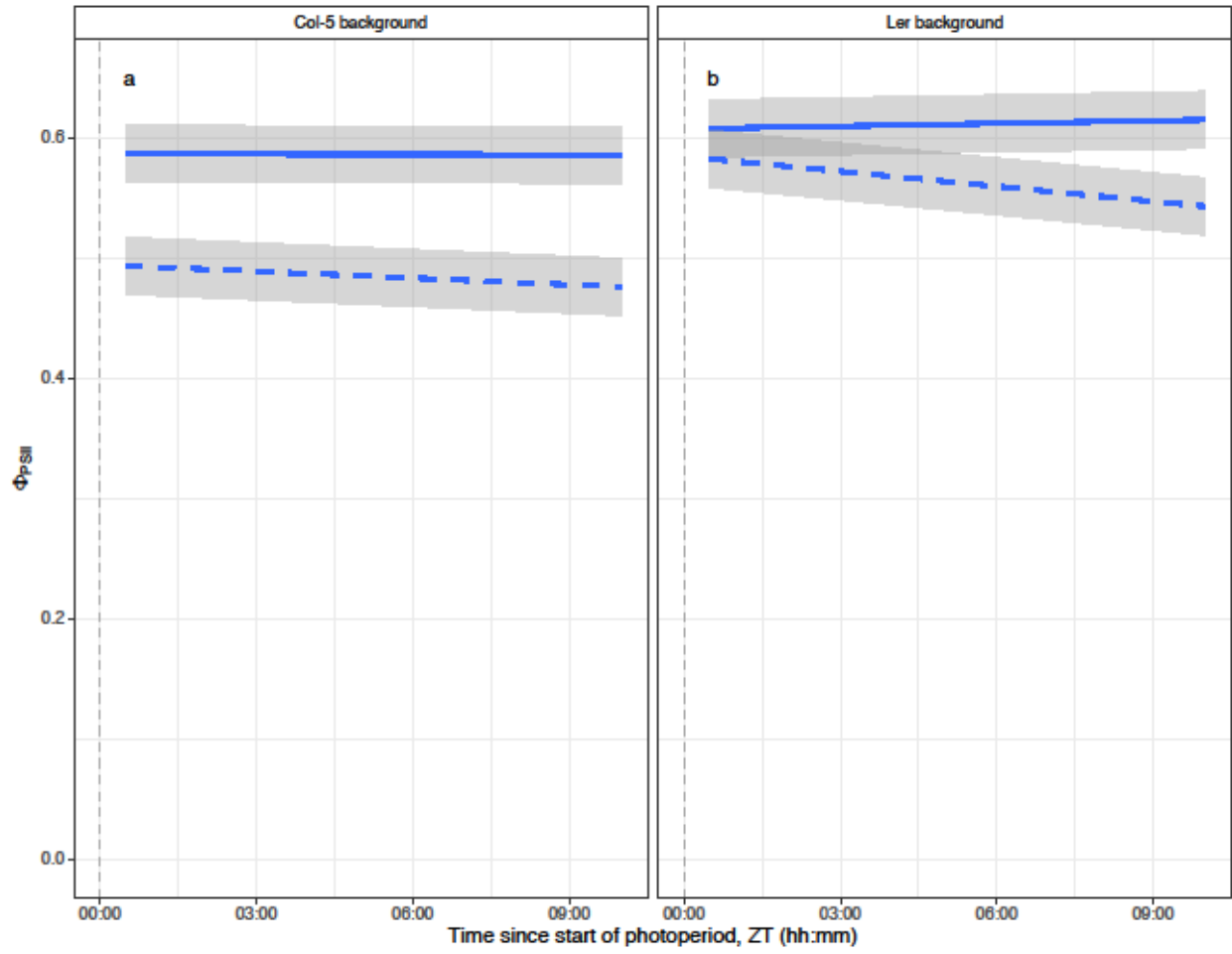
757

758 Fig. 3



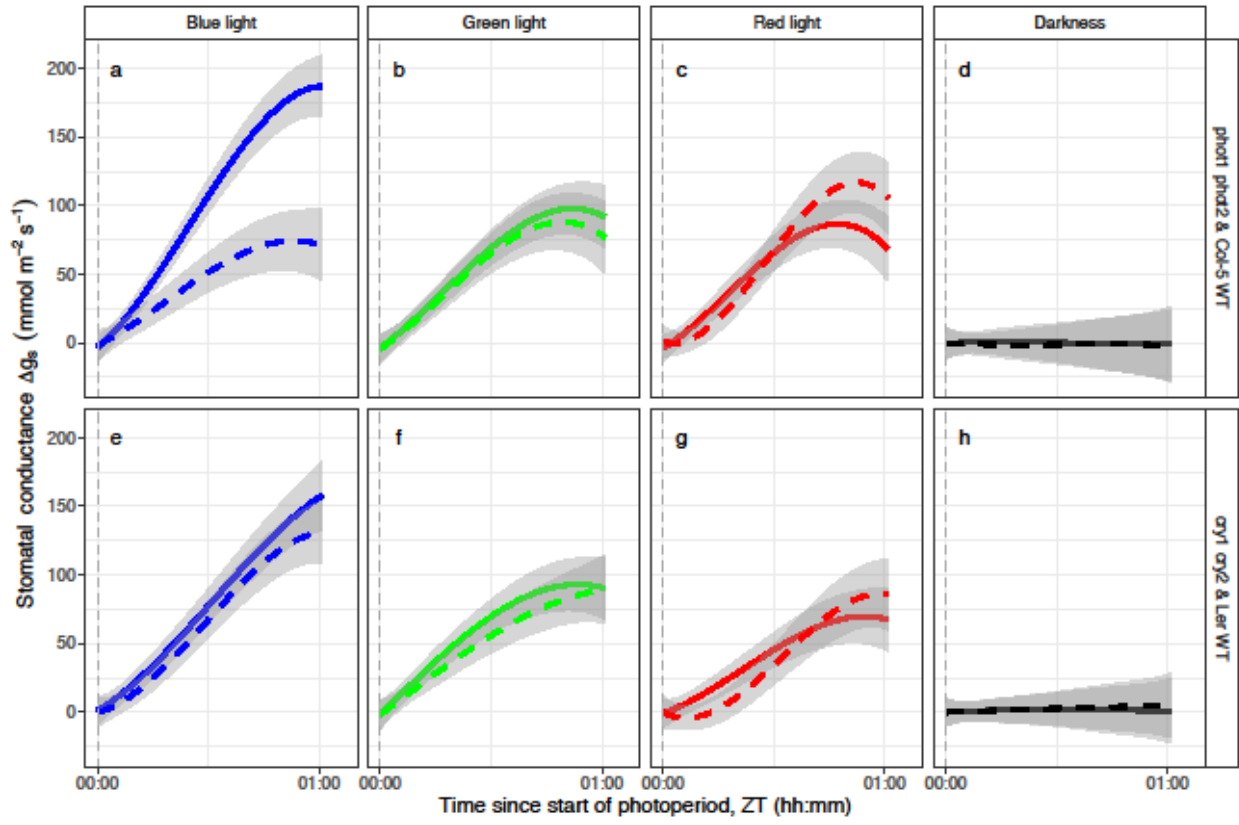
759

760 Fig. 4



761

762 Fig. 5



763